



2011

The Role of T-Type Calcium Channels in Vascular Smooth Muscle Cell Cycle Regulation

Abigail Prier
Loyola University Chicago

Follow this and additional works at: https://ecommons.luc.edu/luc_theses



Part of the [Physiology Commons](#)

Recommended Citation

Prier, Abigail, "The Role of T-Type Calcium Channels in Vascular Smooth Muscle Cell Cycle Regulation" (2011). *Master's Theses*. 573.

https://ecommons.luc.edu/luc_theses/573

This Thesis is brought to you for free and open access by the Theses and Dissertations at Loyola eCommons. It has been accepted for inclusion in Master's Theses by an authorized administrator of Loyola eCommons. For more information, please contact ecommons@luc.edu.



This work is licensed under a [Creative Commons Attribution-Noncommercial-No Derivative Works 3.0 License](#).
Copyright © 2011 Abigail Prier

LOYOLA UNIVERSITY CHICAGO

THE ROLE OF T-TYPE CALCIUM CHANNELS IN VASCULAR SMOOTH
MUSCLE CELL CYCLE REGULATION

A THESIS SUBMITTED TO
THE FACULTY OF THE GRADUATE SCHOOL
IN CANDIDACY FOR THE DEGREE OF
MASTER OF ARTS/SCIENCE

PROGRAM IN CELLULAR AND MOLECULAR PHYSIOLOGY

By

ABIGAIL B. PRIER

MAYWOOD, IL

MAY 2011

Copyright by Abigail B Prier, 2011
All rights reserved.

TABLE OF CONTENTS

LIST OF FIGURES.....	iii
ABSTRACT.....	v
CHAPTER 1: BACKGROUND.....	1
CHAPTER 2: MATERIALS AND METHODS.....	9
CHAPTER 3: RESULTS.....	14
CHAPTER 4: DISCUSSION.....	31
CHAPTER 5: CONCLUSIONS.....	36
CHAPTER 6: FUTURE STUDIES.....	37
BIBLIOGRAPHY.....	38
VITA.....	40

LIST OF FIGURES

	Page
Figure 1. Validation of PASMC cultures for α -Smooth muscle actin	14
Figure 2A. Representative immunostaining of serum stimulated PASMCs for BrdU/S-phase entry at 24 hours	16
Figure 2B. T-type calcium channel subunit mRNA levels in PASMC following serum stimulation	16
Figure 3. Effects of IGF-1 on cellular proliferation	17
Figure 4. Effect of FBS on cyclin D nuclear localization	19
Figure 5. Effects of IGF-1 on Cyclin D nuclear localization	20
Figure 6. Effects of IGF-1 on Ca _v 3.1 and Cyclin D mRNA levels	21
Figure 7. Cytosolic vs Nuclear Cyclin D Fractionation	22
Figure 8. Construction and validation of Adv-cycD-GFP	24
Figure 9. Effect of Mibefradil on cyclin D nuclear translocation	25
Figure 10. Effects of IGF-1 on cyclin D mRNA levels at 8 hours when treated with Adv-Ca _v 3.1sh	26
Figure 11. Effect of Adv-Ca _v 3.1sh on cyclin D nuclear localization	27
Figure 12. Panels of Time Lapse PASMC Adv-cycD-GFP	30

ABSTRACT

Results from previous experiments have provided evidence for T-type channel expression in adult pulmonary artery smooth muscle cells (PASMCs) using electrophysiology and qRT-PCR. Studies have also shown that when T-type channels are blocked, either pharmacological or with small hairpin RNA targeted against T-type channel $Ca_v3.1$ subunit, mRNA levels are reduced and cell proliferation is inhibited. These results suggest a connection between T-type calcium channels and cell proliferation. In this thesis, $Ca_v3.1$ and its possible interplay with cyclin D, an early marker of the cell cycle, was investigated. The time course of cyclin D's translocation to the nucleus to begin the cell cycle was studied and once a baseline was established, the T-type Ca^{2+} channel was knocked down either using a pharmacological blocker, mibefradil, or with shRNA and its effects on the nuclear translocation of cyclin D are presented. Our results suggest that a connection exists between $Ca_v3.1$ and cyclin D in the initiation of the cell cycle.

CHAPTER 1

BACKGROUND

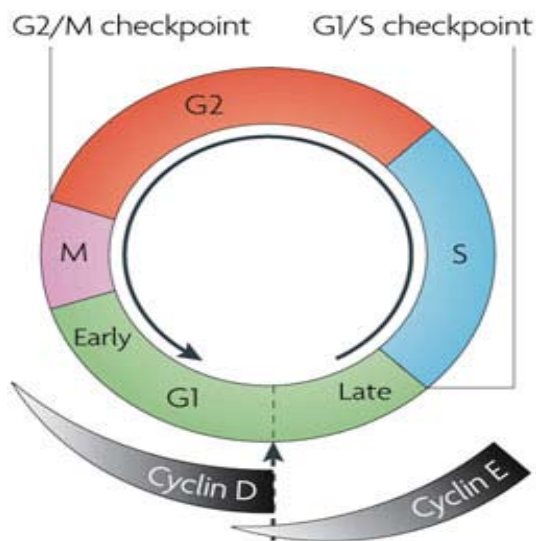
Calcium is a universal second messenger that regulates a number of diverse cellular processes including cell proliferation, development, motility, secretion, learning and memory. Voltage dependent calcium channels are closed during the membrane resting state. Once a cell has become depolarized or excited these channels open and allow an influx of calcium into the cell. Once Ca^{2+} has entered the cell, a plethora of downstream events may occur depending on the type of cells these channels are present in.

While six classes of calcium channels have been identified; P, Q, N, R, T and L, there are two main physiological classes of voltage dependent Ca^{2+} channels, encoded by at least 10 different genes designated as high voltage activated channels, (HVA, Ca_v1 and Ca_v2) and low voltage activated channels (LVA, Ca_v3) (2). The L-type channels, belonging to the HVA family, are found in both excitable and nonexcitable tissue, and they play an important role in normal myocardial and vascular smooth muscle contractility. Multiple subunits (alpha-1, alpha-2/delta, beta, and gamma) make up the L-type channels while T-type channels appear to be comprised of a single alpha subunit encoded by one of 3 genes; $\text{Ca}_v3.1$ (α_{1G}), $\text{Ca}_v3.2$ (α_{1H}), and $\text{Ca}_v3.3$ (α_{1I}).

The importance of Ca^{2+} signaling during the cell cycle has been well established in mammalian cells. Calcium may accumulate intracellularly via two main processes; cytoplasmic Ca^{2+} transients are generated by release of Ca^{2+} from intracellular pools, mainly the sarcoplasmic reticulum (SR) or the endoplasmic reticulum (ER), or by entry of Ca^{2+} from the extracellular environment via Ca^{2+} channels in the plasma membrane. In vascular smooth muscle (VSM), a calcium concentration gradient must be maintained for proper physiologic processes. When the concentration gradient is perturbed, large concentrations of intracellular Ca^{2+} have been found to cause vasoconstriction and even cell death. A normal physiological increase in intracellular Ca^{2+} , 50nM-2 μ M, is required for the initiation and progression of the cell cycle. Spontaneous Ca^{2+} oscillations are observed in the G_0/G_1 phase, at the G_1/S transition, during S phase, and during the exit from mitosis (17). The oscillations seen immediately after cell quiescence have been shown to turn on early genes such as cyclins, which are required for the cell to re-enter the cell cycle (3). During the G_2/M phase of the cell cycle, the Ca^{2+} is involved in the break down of the nuclear envelope and subsequent division of the cell. The regulation of intracellular calcium is especially important for cell proliferation and hypertrophy. For example, it has been shown that the depletion of intracellular inositol 1,4, 5-triphosphate-sensitive Ca^{2+} stores by thapsigargin, a pharmacological agent which blocks the calcium ATPase on the ER resulting in Ca^{2+} depletion in the ER, resulted in a halt of cell division (19).

Once calcium levels are sufficient to turn on the early genes, such as cyclin D1, the cell cycle may progress. There is a highly conserved family of serine/threonine cyclin

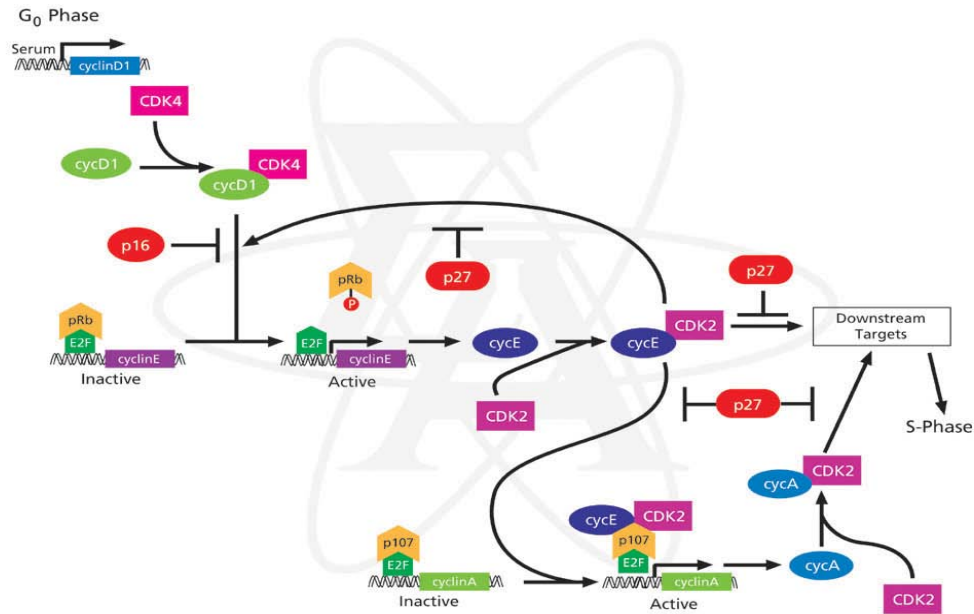
dependent kinases (CDKs) that become activated upon binding to cyclins. Progression of the cell cycle is dependent upon relative levels of individual cyclins. Members of the cyclin D family are known as G1 phase cyclins and upon binding to CDK4 regulate the transition of cells from the G0 phase into the G1 phase. Cyclin E family members, synthesized during late G1 phase, bind to CDK2 and promote the onset of DNA replication during the G1/S phase. Finally cyclin B members are known as the M phase cyclins and are synthesized during G2. They pair with CDK 1 and their pairing leads to the assembly of characteristic M phase components such as the spindle fibers (8, 18).



Orford, K, *Nature Reviews Genetics* 2005; 9: 115-128

Components of the cyclin D family are particularly important for signaling cell cycle entry, or the G0/G1 transition (12). Cyclin D1/CDK4 activity is kept in check by several distinct regulatory events. One regulatory protein implicated in the calcium dependent mechanisms of cyclinD/CDK regulation is calmodulin (CaM). Calmodulin is a ubiquitously expressed calcium binding protein that recent studies have shown to play a

pivotal role in the regulation of cell cycle progression (8). Calmodulin is a 148 amino acid long protein composed of four electronegative calcium binding pockets. CaM is able to bind the extracellular calcium following their influx through calcium channels as well as calcium from the intracellular pools, the endoplasmic and the sarcoplasmic reticulum. Once the four pockets are bound with calcium, CaM acts as a signal transducer turning electrical signals into biological signals that regulate numerous downstream cascades within the cell. Two potential targets for CaM during the initiation of the cell cycle include its interaction with Ca^{2+} /CaM-dependent protein kinases (CaMKs) and the interaction with calcineurin; however, the manner in which these proteins interact to regulate the cell cycle remains unknown (5). Recent studies have implicated CaMKII function early in G1 phase as a regulator of cyclin D/cdk4 activation by pharmacologically blocking CaMK activity. These studies showed cellular arrest in the G₀ phase (16). In addition to CaMKII regulation or as an alternative mechanism, cyclin D/CDK4 is subjected to growth factor dependent post-translational regulation. Once the cyclin D/ CDK complex is assembled it requires phosphorylation by the CDK-activating kinase (CAK). Upon phosphorylation by CAK the complex translocates to the nucleus where it initiates its primary role, phosphorylating the retinoblastoma protein (Rb) (7). Once Rb is phosphorylated by the complex, E2F transcription factors are freed and are able to bind to the promoter sequence of the target genes for the progression of the cell cycle (4,10).



Regulatory cascade of cyclin gene expression, from www.sigmaaldrich.com

There is still much to elucidate in the regulation of calcium, the cyclinD/CDK4 complex and their role in the initiation of the cell cycle. Our lab and others have shown the effects of mitogenic agents, fetal bovine serum (FBS) and insulin-like growth factor-1 (IGF-1), both on the proliferation and the expression of T-type Ca^{2+} channels in a variety of cell types (work unpublished).

Previously it was thought that T-type channels were primarily limited to fetal or neonatal cardiac muscle cells; however, T-type Ca^{2+} currents were reported in one study with long standing pressure overload-induced hypertrophy in adult feline heart (15). Thus, electrophysiological analysis provided evidence that T-type channels may be re-expressed in association with cardiac injury. This experiment did not clarify a role for T-

type channels in the injury response. More recent experiments have provided data to bolster the evidence of T-type channel involvement during injury response (14). Neonatal rat ventricular myocytes (NRVM) were isolated and cultured. The cells were allowed 48 hours quiescence with 0% serum and then 20% serum was introduced for 24 hours. The cells that were exposed to the serum displayed evidence of hypertrophy. These cells as well as control, 0% serum, were then treated with known pharmacological T-type and L-type calcium channel blockers, mibefradil and verapamil. These blockers caused a dose-dependent reduction in cell hypertrophy, and the inhibitory action of mibefradil alone suggested that T-type channels played a role in the cell injury response, since this drug is selective for T-type over L-type calcium channels (1).

Our laboratory and others have shown a correspondence between the expression of T-type Ca^{2+} channels in neonatal rat ventricular myocytes (NRVM) and vascular smooth muscle cells (VSMC) with stages of proliferation, such as after an injury or in pathological conditions (2,14). In one study, NRVM were serum starved, then exposed to 7% fetal bovine serum (FBS), which resulted in an approximately 2-fold upregulation of $\text{Ca}_v3.1$ subunit mRNA after 72 hours (Figure 2). Similar NRVM cell cultures were also stained with bromodeoxyuridine (BrdU), a marker of cell cycle and DNA synthesis. There was a marked increase in the number of cells in the S-phase after serum addition, providing evidence that with the addition of serum to the cell medium cells were proliferating.

Finally, a recent study has reported developmental intimal thickening of the pulmonary artery and the descending aorta, which involves VSMC proliferation and cellular migration. An interesting observation was made when VSMC samples were treated with kurtoxin, a selective T-type channel blocker that binds with high affinity to the alpha 1G, Ca_v3.1 subunit and modifies the channel by inhibiting the voltage-dependent gating mechanics. Thymidine [³H] incorporation and BrdU staining were decreased suggesting that T-type Ca²⁺ channels are involved in smooth muscle cell proliferation (21). To further investigate the theory of T-type channel involvement in cellular proliferation an experiment was done by Dr. Florentina Pluteanu in our lab which knocked down Ca_v3.1 using Adv-Ca_v3.1sh in VSMC. This method blocks the expression of the alpha (pore-forming) subunit of the channel and LVA Ca²⁺ currents. Adv-Ca_v3.1sh treated VSMC samples were collected and analyzed using qRT-PCR to ensure a proper knock down of the T-type channels. VSMC cell cultures were also stained with cyclin D1 antibody to determine cyclin expression and intracellular (nuclear vs. cytoplasmic) localization. Preliminary data suggest that in Adv-Ca_v3.1sh treated cells, cyclin D seems to be arrested within the cytoplasm suggesting that T-type channels play a key role in the movement and subsequent localization of cyclin D into the nucleus. These studies indicate a correlation between Ca²⁺ influx through T-type channels and the movement of cyclin D into the nucleus to initiate the cell cycle. If the direct interaction between calcium influx through T-type channels and cyclin D nuclear translocation can be

determined, then T-type channels might become a therapeutic target for pathological vascular myocyte proliferation and/or migration.

CHAPTER 2

MATERIALS AND METHODS

PASMC Culture

Sprague Dawley rats (200-250 g) are anesthetized with xylazine and ketamine; heart and lung are removed and kept in cold low calcium physiological saline solution (PSS). Intralobular arterioles (3rd and 4th branches) are dissected, cleaned of adventitia and enzymatically dissociated in 2 steps: one incubation in 1 mg/ml collagenase (Roche Scientific, USA) for 20 min at 37°C (to remove the remaining adventitia and endothelial cells) followed by a second step of 2 mg/ml collagenase and 0.5 mg/ml elastase (Roche Scientific, USA) for 60 min at 37°C, followed by trituration and centrifugation 5 min at 1000 rpm. Cells are resuspended in Smooth Muscle Basal Growth Medium (Clonetics Corp., USA) and cultured in 35 mm dishes. After 3-5 days, when spindle cells start to appear, the medium is changed to low serum (0.1 %) in order to remove the fibroblast contamination. After 3 days, 5% serum is added back. When the cells reach a 90% confluent layer, they are split and prepared for experiments. The purity of the culture is tested by smooth muscle α -actin immunostaining. Rat PASMC are used from passage 4 to 10. The cells used for the preliminary data have shown a minimum 90% α -actin-positive cells.

FBS studies- PASMCs were plated in 6 well, on 12mm cover slips coated with gelatin, or in 100mm plates and allowed to settle for 24 hours in Smooth Muscle Basal Growth Medium. Cells were then arrested for 48 to 72hrs in Dulbecco's Modified Eagle Medium in order to (Invitrogen) in order to synchronize cells in the G₀/G₁ phase of the cell cycle. After the arrest 10% FBS was added back into the medium.

IGF-1 studies- PASMCs were plated in 6 well dishes or on 12 mm cover slips coated with 0.2% gelatin. Once the cells reached the desired confluency they were arrested for 48 hours to obtain synchronization. After the 48 hour period 10 μ M IGF-1 was added to DMEM and the cells were incubated until desired time points.

Mibefradil studies- PASMCs were plated on 12mm cover slips coated with .2% gelatin and allowed to settle for 24 hours. Mibefradil (Tocris) was added to the cells at a concentration of 10 μ M and allowed to incubate for 20 minutes. Following the initial incubation time treatments were administered.

Immunostaining

PASMC grown on cover slips are fixed in 4% paraformaldehyde/PBS for 20 minutes and are then incubated in blocking buffer (1% goat serum/PBS/0.1% Triton X-100) for 1 hour at room temperature on a rocker. Primary cyclin D1 and cyclin B antibodies (Sigma) are added at a 1:100 dilution in blocking buffer and placed on rocker for 1hr. The cyclin E primary antibody (Santa Cruz Biotechnology) is diluted at 1:100 with blocking solution. Secondary antibodies, Alexafluor series, are obtained from Invitrogen and are used at a

1:200 dilution. The samples are left to incubate in the secondary for at least an hour. The cell cover slips are then mounted using Prolong Gold with DAPI from Invitrogen.

Western Blot

Plasmid vector containing cyclin-GFP fusion protein is used to transfect HEK cells using Lipofectamine from Invitrogen. Cells are harvested with lysis buffer from Qiagen and equal amounts of protein and run on 12% polyacrylamide gel. The proteins are transferred onto nitrocellulose membranes. Blots are blocked with 5% reconstituted powdered milk (Carnation) for 1.5 hours. Primary cyclin D1 (Cell Signaling Technologies and Sigma), anti-GFP (Sigma), α smooth muscle actin (Sigma), and Lamin A/C (Cell Signaling) antibodies are diluted 1:1000 in TBS-T (10mmol/L Tris [pH 8.0], 150mmol/L NaCl, and 0.05% Tween-20). Primary antibodies are added and incubated on a rocker at 4°C overnight. Secondary antibodies were purchased from Pierce and applied to samples in a 1:1000 dilution. After rinsing with TBS-T, immunoblots are processed for ECL detection using ECL Western Blotting Analysis system by GE Healthcare. Cytoplasmic vs nuclear fractionation was accomplished using NE-PER Nuclear and Cytoplasmic Extraction Reagents (Pierce), according to the manufacturer's protocol.

qRT-PCR

Total RNA is isolated from rat pulmonary artery smooth muscle cells using Sidestep Lysis Stabilization Buffer from Stratagene. The cDNA is reverse transcribed using iScript from Biorad. The samples are subjected to real time PCR in a reaction containing SYBR Green Master Mix and gene expression primer assays from SuperArray. 18s ribosomal

RNA assay is used as an internal control to normalize for variable RNA concentrations (SuperArray). All reactions are conducted on an Applied Biosystems 7300 Real Time PCR system according to the manufacturer's protocol. Relative quantification data are generated by the $\Delta\Delta C_t$ method using RQ software (Applied Biosystems). The primers are validated for high efficiency (97-100%) and specificity before running the samples.

CyclinD-GFP fusion protein

Full length human cyclin D cDNA clone was obtained from Origene. The primer design program Oligo was used to design forward and reverse primers to amplify the cyclin D coding region, using the cDNA as the template (forward primer: 5' TGCCCAGGAAGAGCCCCAGCC 3' and reverse primer: 5' ACGTCGGTGGGTGTGCAAGCC 3'). The designed primers are ordered from Integrated DNA Technologies. The human cyclin D coding region is amplified, gel purified (Qiagen gel purification kit) and subcloned into a TOPO-TA vector (Invitrogen), which is then subcloned upstream and in frame with green fluorescent protein (GFP) into the pEGFP-N1 vector (Clontech). The cyclin-GFP fusion is then cloned into pShuttle-CMV (Stratagene) for adenovirus construction. pShuttle cyclin-GFP construct is electroporated into BJ5183 cells expressing adenovirus vector AdEasy (Stratagene) and colonies containing the recombinant adenovirus are identified and isolated. The construct is then digested with Pac1 (New England Biolabs) and is used for transfection of HEK 293 host cells to produce the recombinant adenovirus. The fusion was sequenced for confirmation.

RNA Interference

siRNA target finder software (Ambion) was used to first identify siRNA target sequences for inhibition of $Ca_v3.1$. The most effective target sequence was selected previously by validation using psiCHECK™-1 vector/luciferase reporter system (Promega). This target sequence was extended to a 29 base pair sequence that was incorporated into a small hairpin RNA (shRNA) construct for $Ca_v3.1$ inhibition. shRNA-encoding primers (Integrated Data Technologies) were cloned into a fluorescent-tagged expression vector (pSilencer DsRed express, Clontech). $Ca_v3.1$ shRNA adenovirus is then constructed as described in Ambion's Silencer siRNA construction kit. A negative control adenovirus was constructed in a similar fashion using scrambled siRNA target sequence. These reagents were constructed previously and $Ca_v3.1$ knockdown was validated in the Cribbs laboratory.

Time Lapse Fluorescent Microscopy

Nikon Diaphot inverted microscope was used to acquire time lapse images of PASMCS infected with Adv-cycD-GFP. PASMCS were plated on 15mm cover slips coated with 0.2% gelatin and allowed to reach 70% confluency. The cells were then arrested for 48 hours in serum free DMEM. After the 48hour arrest, DMEM supplemented with 10% FBS was added to the culture and allowed to incubate for 3 hours until placed in a chamber placed on a stage heater set at 37°C. Cells were continually bathed with heated HAM's F-12, with L-glutamine (Mediatech) and 10% FBS. Simple PCI image processing system was used to acquire the image.

CHAPTER 3

RESULTS

Specific Aim 1. Characterize the expression and activation of intracellular cyclin D in proliferating vascular smooth muscle cells.

Validation of culture. In order to validate our cultures as smooth muscle cells, PSMCs were plated and fixed on 12mm cover slips. Cultures were immunostained with a monoclonal antibody against α smooth muscle actin, which confirmed our cultures were comprised of smooth muscle cells (Figure 1).

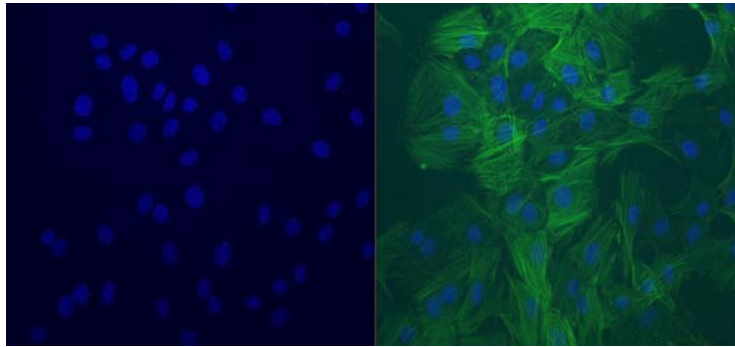


Figure 1. Immunostaining of PSMC cultures for α -Smooth muscle actin. Cultured PSMCs passage 6 were fixed with 4% paraformaldehyde/PBS, permeabilized with 0.5% Triton X-100 and stained with monoclonal antibody against α -SM actin at a dilution of 1:5000. Blue indicates DAPI staining of the nuclei while Alexafluor green 488 stain is for α -SM actin. The first panel is DAPI stain alone while the second panel is an overlay of smooth muscle actin and DAPI.

PASMC proliferation and T-type channels. Previous studies done in our lab by Dr F. Pluteanu have shown PASMC cultures proliferate with serum stimulation. PASMCs were plated on 12 mm cover slips, arrested, then stimulated with 5% FBS. PASMCs were incubated over night at 37° C either with serum or with no serum. Cells were fixed at 24 hours, permeabilized, and treated with 2N HCl for 15 minutes to denature the DNA and expose the epitopes to the BrdU antibody. Cells in the S phase of the cell cycle were indicated by immunostaining for BrdU (Figure 2A). To further study the effects of serum stimulation on the T-type channel, PASMCs were plated in 6 well dishes, allowed to settle for 24 hours, and then arrested for 48 hours to allow for the cells to synchronize. 5% FBS was then added back to the medium and samples were collected at 24, 48, 72, and 96 hours post serum addition. mRNA samples were isolated and probed with T-type subunits Ca_v3.1 and 3.2. mRNA levels of Ca_v3.2 remain relatively unchanged while Ca_v3.1 level is increased ~4 fold by 96 hours post stimulation (Figure 2B). qRT-PCR results indicate a 2-fold increase in Ca_v3.1 at 48 hours post stimulation (p<.001). Average relative quantification of Ca_v3.1 at time 24 is 1.13±.36 whereas at time 48 RQ value is 3.49±.49. Cyclin D RQ at 24 hours is 1.26 and at 48 hours it is 2.61 (also measured by Dr. Pluteanu, not shown).

A similar study was performed by Dr Pluteanu using IGF-1 as the mitogenic factor. Labeling of the cells with BrdU indicated that IGF-1 stimulated cell proliferation, and qRT-PCR results indicated a 2-fold increase in Ca_v3.1 at 48 hours post stimulation (p<.001) (Figure 3A and B). These data indicate that PASMCs in culture can be

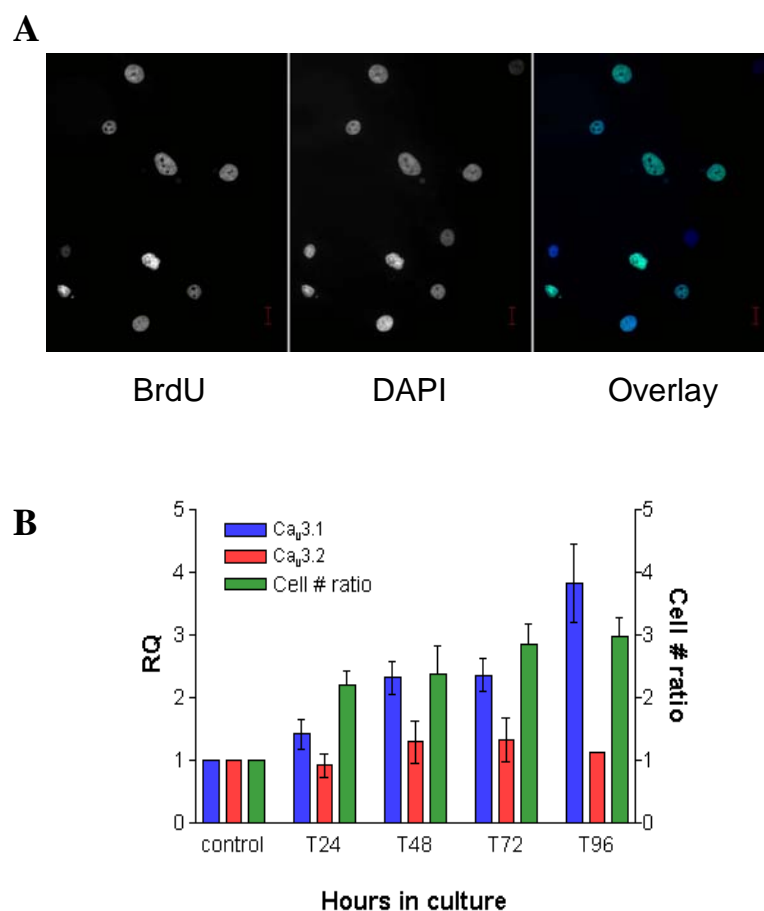


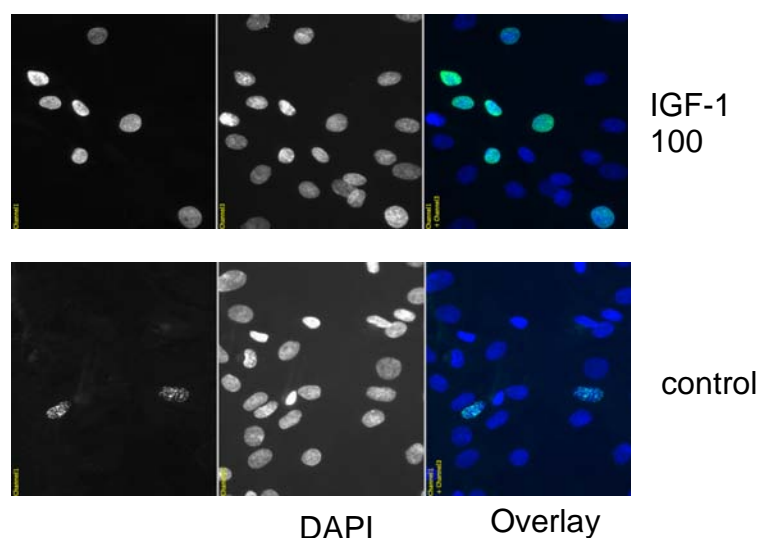
Figure 2. (A) Representative immunostaining of serum stimulated PSMCs for BrdU/S-phase entry at 24 hours. PSMCs were incubated overnight with BrdU (Invitrogen), fixed, permeabilized, treated with 2N HCl to denature DNA and expose epitopes, and stained with monoclonal anti-BrdU@488 antibody (1:50) and nuclei counterstained with DAPI. Scale bar =10 μ m.

(B). T-type calcium channel subunit mRNA levels in PSMC following serum stimulation. Cells were plated in 6 well plates, arrested, and stimulated with 5% FBS. mRNA samples were isolated and qRT-PCR was carried out for T-type subunits Ca_v3.1 and 3.2. mRNA levels of Ca_v3.2 remain relatively unchanged. Ca_v3.1 is increased ~4 fold by 96 hours post stimulation. Cell # ratio is derived from MTT assay.

stimulated to enter the cell cycle and proliferate and at the same time Ca_v3.1 mRNA is upregulated. Based on these results, subsequent experiments were designed to investigate

whether the $\text{Ca}_v3.1$ T-type Ca^{2+} channel interacts with cyclin D signaling as an early step in cell cycle progression.

A



B

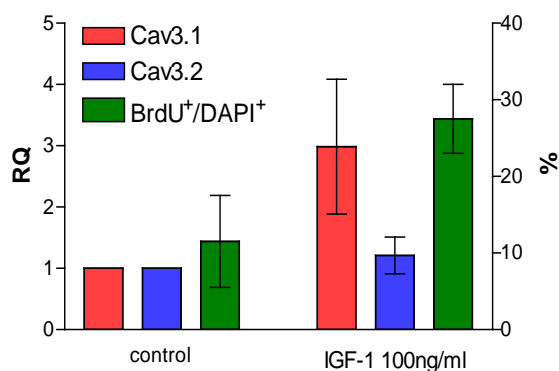


Figure 3. Effects of IGF-1 on cellular proliferation.

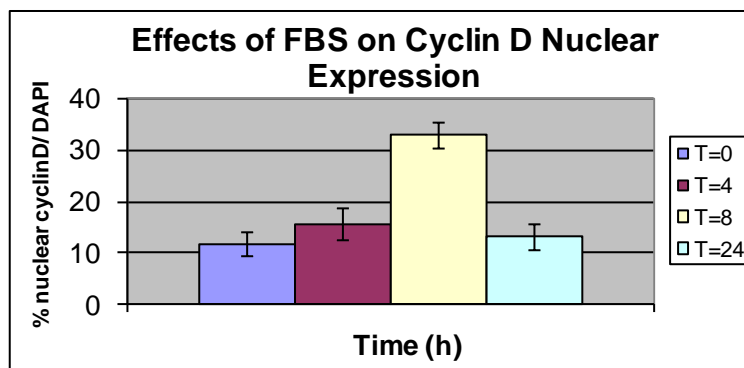
(A) Samples collected 24 hours after stimulation. Representative immunostaining of PSMCs were incubated over night with BrdU (Invitrogen), fixed, permeabilized, and treated with 2N HCl to denature DNA and expose epitopes. PSMCs were then stained with monoclonal anti-BrdU@488 antibody (1:50) and nuclei counterstained with DAPI. Scale bar is 10 μm .

(B) Graph represents PSMCs relative mRNA levels of the $\text{Ca}_v3.1$ and 3.2 T-type subunits. BrdU⁺/DAPI⁺ was calculated by dividing the number of BrdU positive cells by the number of DAPI cells. Quantity given as a percentage.

Cyclin D and mitogenic factors. It remains unknown as to the time course of cyclin D translocation to the cell nucleus in order for the cell cycle to begin and therefore, studies were done to characterize intracellular cyclin D expression in stimulated PASMOC cultures. PASMOCs were plated on 12 mm cover slips, allowed to settle for 24 hours, and then arrested for 48 hours. After the arrest, 10% FBS was added back to the medium. Cells were fixed for immunostaining at 0, 4, 8, and 24 hours post stimulation. Immunostaining indicated that cyclin D translocation occurs by 8 hours post FBS addition. At 8 hours more than 30% of cells within a PASMOC population expressed cyclin D within the nucleus compared to 10% at 0 hours (Figure 4A), indicating that the cells were entering in the cell cycle from the quiescent phase. At 24 hours the percent of cells with nuclear cyclin D is similar to time 0, 11.8%, suggesting that the cells have progressed through an entire cell cycle. This interpretation is consistent with previous cell counts showing a doubling of cell number at 24 hours after serum stimulation (Dr. F. Pluteanu, Figure 2). After 4 hours stimulation, cyclin D intensity was relatively weak and diffuse throughout the cell, while at 8 hours the signal was more robust and found within the nucleus. Although cyclin D appears to be present in the cells at 24 hours, it is not significantly expressed within the nucleus (Figure 4B).

The same type of experiment was carried out using IGF-1 as the mitogenic factor and similar results were obtained. At 8 hours post IGF-1 addition more than 30% of the population showed cyclin D nuclear expression. Total cell counts based on DAPI-positive nuclei showed that by 24 hours cell counts showed that the number of cells within the

A



B

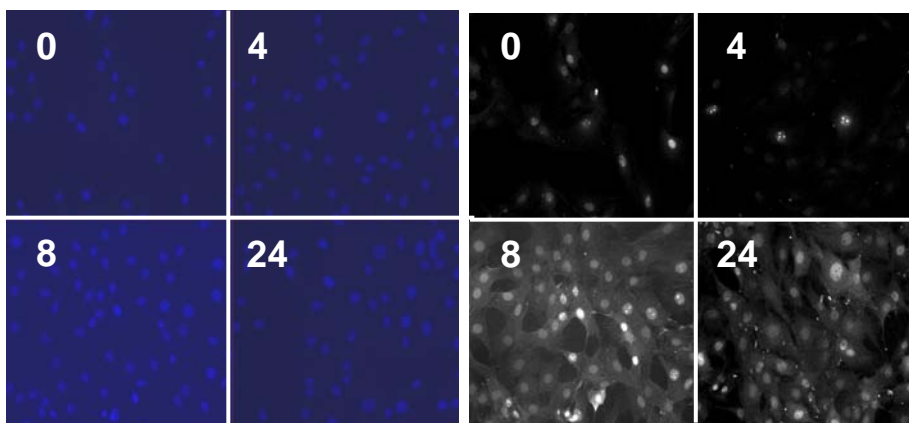


Figure 4. Effect of FBS on cyclin D nuclear localization.

(A) Graph represents an n=4 studies from different passage numbers 5-9. PSMCs were plated on 12mm cover slips, arrested, and stimulated with 10% FBS. Samples were fixed and stained with monoclonal antibody against cyclin D (Sigma) at a dilution of 1:400 at 0, 4, 8, and 24 hours post stimulation. Secondary antibody was AlexaFluor 488 and nuclei were stained with DAPI.

(B) Immunostaining panel on the left represents DAPI stain while right panel is cyclin D expression. Photos were taken of different fields and the number of DAPI positive cells was counted. For the percentage of cyclin D nuclear expression, the number of positive nuclear cyclin D was divided by the total number of DAPI positive cells. SEM was found by taking the percentage of nuclear expression/DAPI for each field and comparing to average value for all fields. Values- T=0 12.3 ± 2.3 , T=4 15.1 ± 3.3 , T=8 33 ± 2.7 , T=24 12.8 ± 2.4 . Bottom panel A=T0 B=T4 C=T8 D=T24 hours post FBS stimulation. Images were taken at equal intensities and equal exposures. These samples were also stained in parallel.

population had doubled (Figure 5). Cell count was determined by taking images of 8 fields on cover slips and counting the number of DAPI+ cells per field (data not shown).

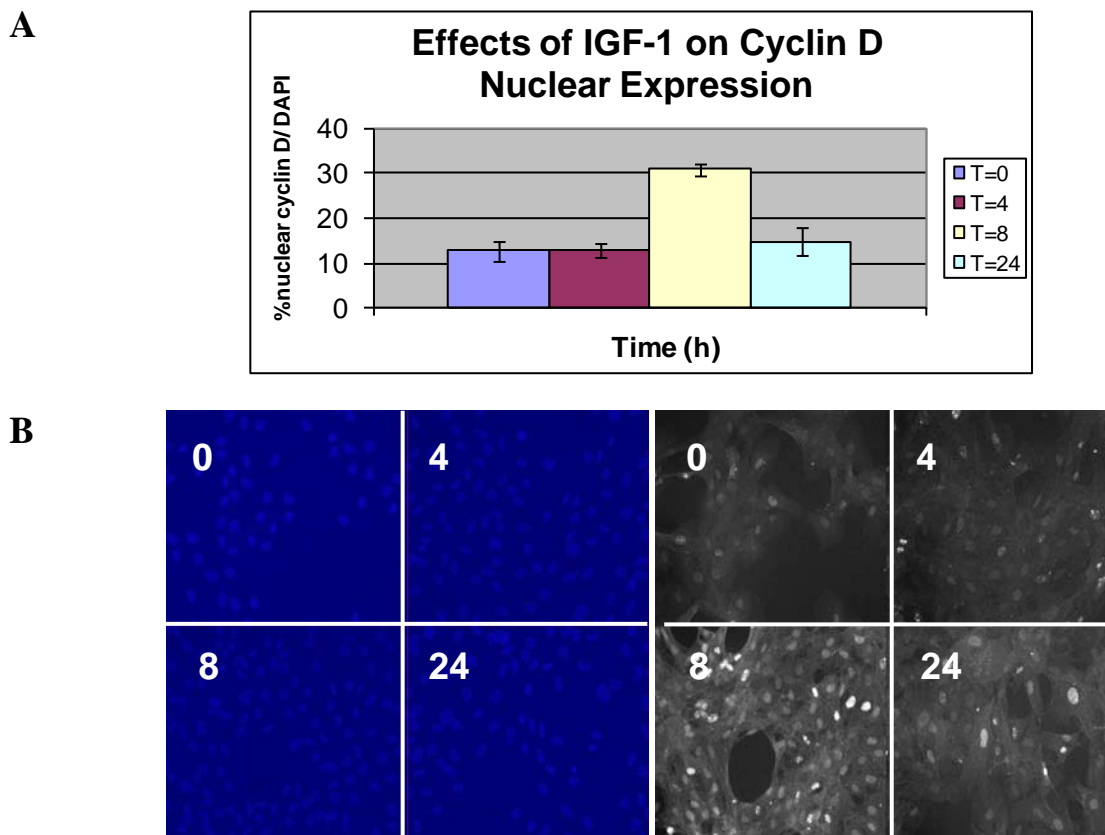


Figure 5. Effects of IGF-1 on Cyclin D nuclear localization.

(A) Graph represents n=4 studies from different passage numbers 5-9. Conditions were the same as stated in Figure 4 but cells stimulated with 100ng/ μ L IGF-1. SEM values- T=0 11.9 \pm 2.4, T=4 12.1 \pm 1.5, T=8 31.2 \pm 1.1, T=24 14.8 \pm 3.0.

(B) Representative micrographs of nuclear DAPI (blue) and cyclin D fluorescence in IGF-1 treated PSMCs at the indicated time points.

To determine the transcriptional regulation of cyclin D, qRT-PCR was performed to examine the expression of cyclin D mRNA following stimulation with IGF-1. For

these experiments, the same samples were used to measure the expression of cyclin D mRNA by qRT-PCR that had been previously evaluated for $Ca_v3.1$ expression by Dr. F. Pluteanu (as shown in Figure 3). Populations were grown in 6 well plates, arrested, stimulated, and the mRNA was isolated at 24 and 48 hours post IGF-1 addition. At 24 hours post IGF-1 treatment there was a slight but insignificant increase in cyclin D mRNA levels. By 48 hours, cyclin D levels were increased by ~2.5 fold as compared to time 0 ($p=.382$). As shown in figure 6, IGF-1 increased $Ca_v3.1$ mRNA levels by almost 3.5-fold which is significant ($p<.001$). The increase in both $Ca_v3.1$ and cyclin D mRNA levels may indicate a role for $Ca_v3.1$ in the regulation of cyclin D.

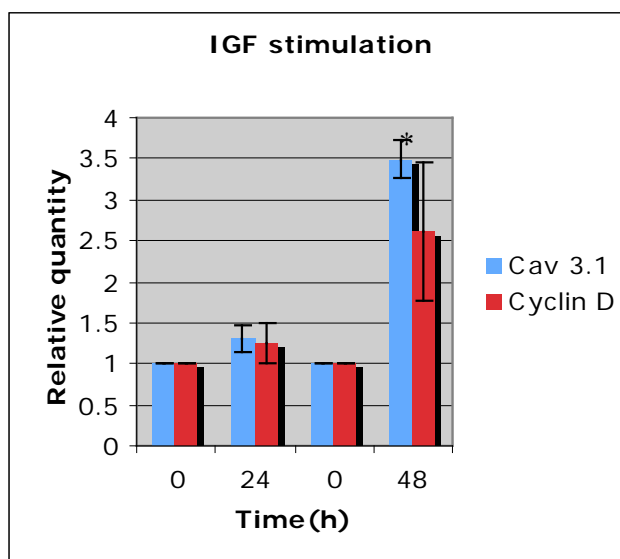


Figure 6. Effects of IGF-1 on $Ca_v3.1$ and Cyclin D mRNA levels. PSMCs were grown in 6 well plates, arrested, stimulated with 100 ng/ μ L of IGF-1, and the mRNA was isolated at 24 and 48 hours post IGF-1 addition (Dr Pluteanu). qRT-PCR was run using SYBR green (Fermentas) and probed with $Ca_v3.1$ (Super Array) and Cyclin D (Super Array). Error bars are standard error of the mean. $Ca_v3.1$ 24 hrs SEM. $1.37 \pm .17$. Cyclin D 24 hrs SEM $1.31 \pm .24$. $Ca_v3.1$ at 48 hrs SEM $3.48 \pm .23$. Cyclin D at 48 SEM $2.63 \pm .09$. ($p=.38$ cyclin D) ($***p<.001$ $Ca_v3.1$) Statistics from one way ANOVA.

To further explore the time course of cyclin D localization Western blot analysis was performed. Cell cultures were collected and fractionated, separating the nuclear components from the cytosolic. The samples were collected at time 0, 4, 8, and 24 hours post FBS stimulation. Equal amounts of protein were loaded and the blots were probed with cyclin D, lamin A/C (nuclear protein) as well as α smooth muscle actin, as a control for protein loading. Lamin served as a marker of fractionation purity (Figure 7).

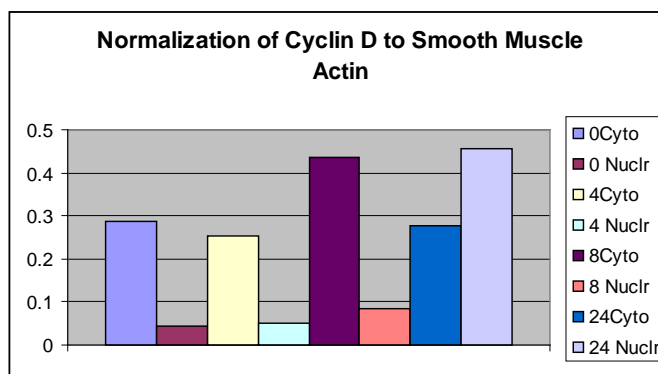
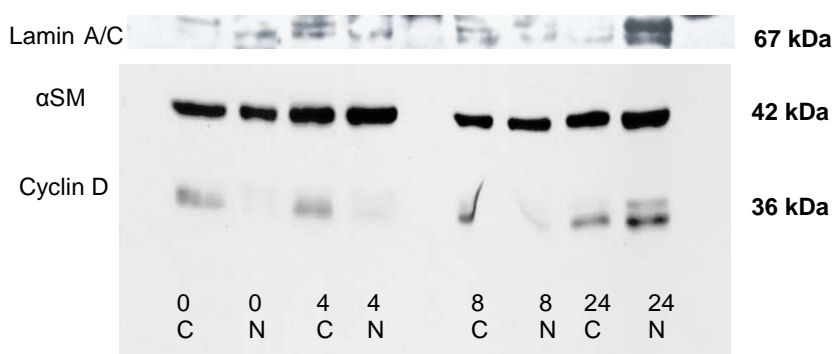


Figure 7. Cytosolic vs Nuclear Cyclin D Fractionation.

N=1 PSMCs passage 8 were grown in 100mm dishes (Falcon). Cultures were plated, arrested, and stimulated with 10% FBS. Samples were harvested and components were isolated at 0, 4, 8, and 24 post FBS addition as stated by manufacture's protocol (Pierce). Lamin A/C (Cell Signaling) was used as a marker of nuclear components at a concentration of 1:1000. α Smooth muscle actin was run as the normalization at 1:1000. Cyclin D was used at a concentration of 1:400 and lanes were normalized to α SM actin. Densitometry was performed and normalization was calculated by dividing the total pixels in each cyclin D lane by the total number of pixels in α SM actin.

Cyclin D runs at 36kD and is expressed in all lanes while lamin is seen as a doublet at 67kD and 62kD and actin at 42kD. Densitometry was performed on the bands and normalization was achieved by dividing cyclin D by α smooth muscle actin signal (Figure 7 graph). The presence of lamin in cytoplasmic lanes indicates that the fractionation was not entirely pure. Results do indicate that nuclear cyclin D was increased compared to cytoplasmic cyclin D at 24 post FBS stimulation.

GFP-tagged cyclin D adenovirus reagent. To visualize the intracellular localization of cyclin D in PSMCs and its possible regulation by $\text{Ca}_v3.1$ T-type Ca^{2+} channels, a cyclin D-GFP fusion protein was constructed and incorporated into an adenoviral vector, to allow high efficiency expression of cyclin D-GFP in PSMCs. Figure 8A outlines the construction of Adv-cyclin-GFP. The proper construction of the Adv-cycD-GFP was confirmed by Western blot (Figure 8B). Cyclin D positive staining is seen for both cyclin D control plasmid (~36kD) and cyclin D-GFP fusion (larger size due to the fusion protein), where no plasmid or GFP lane are negative for cyclin D. On the other hand, GFP antibody revealed a band in the GFP and fusion lanes, but not cyclin D or no plasmid lanes. These gels indicate that the fusion construct led to the production of intact cyclin D and GFP proteins.

Specific Aim 2. Determine the relationship between T-type calcium channels and cyclin D activation in proliferating vascular smooth muscle cells.

$\text{Ca}_v3.1$ Knockdown in PSMC. Once the movement and the time course of nuclear

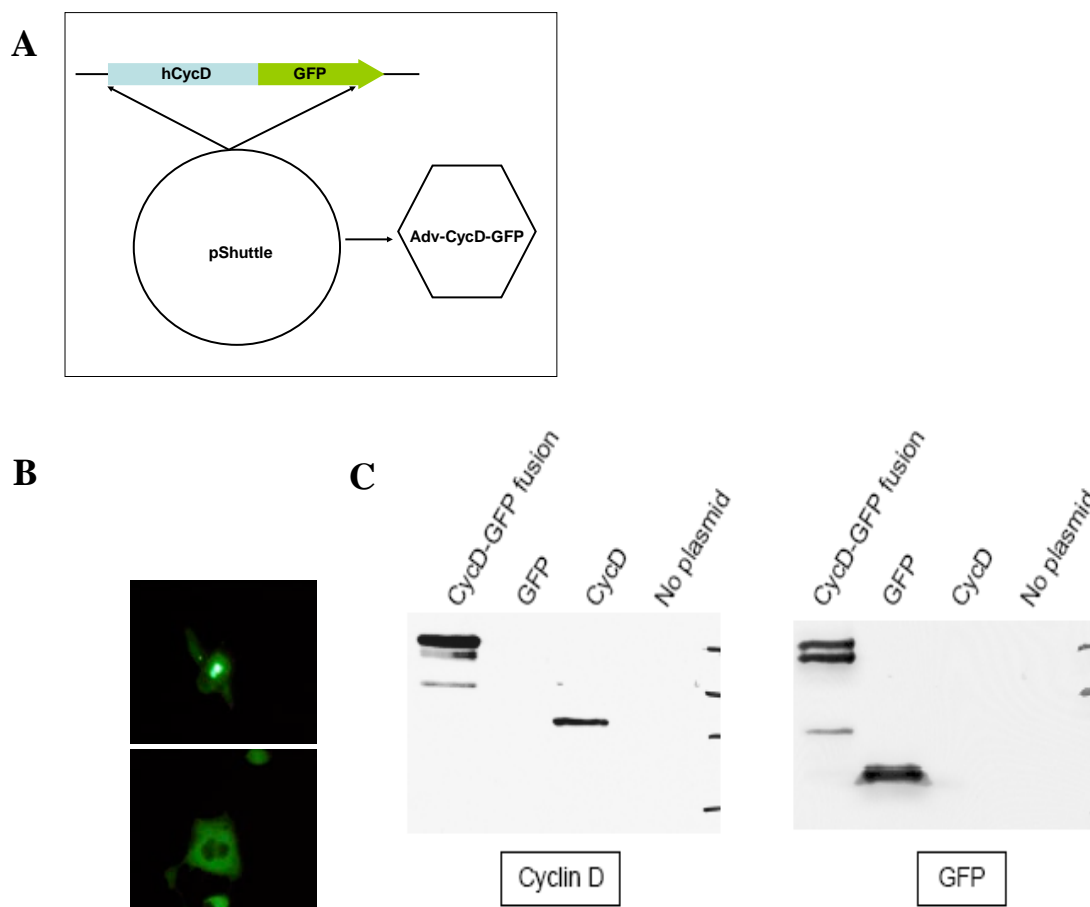


Figure 8. Construction and validation of Adv-cycD-GFP.

(A) Schematic of Adv-cycD-GFP construction.

(B) 60mm dishes of HEK cells were infected with Adv-cycD-GFP and GFP plasmid alone to confirm that GFP alone is not found within the nucleus. Photos taken at a magnification of 20X.

(C) Western Blot of Adv-cycD-GFP. 2 gels run with Fusion, Cyclin D, GFP, and plasmid. The gel marked cyclin D was blotted with cyclin D primary antibody (1:400) while blot GFP was probed with GFP antibody(1:1000). Cyclin D positive staining is seen for both cyclin D control plasmid (~36kD) and cyclin D-GFP fusion (larger size due to the fusion protein), where no plasmid or GFP lane are negative for cyclin D. On the other hand, GFP antibody a band in the GFP and fusion lanes, but not cyclin D or no plasmid lanes.

localization had been established we sought to determine the relationship between T-type calcium channels and cyclin D activation in proliferating vascular smooth muscle cells. Our previous studies may suggest some type of partnership based on the evidence provided by the PCR results. As the $Ca_v3.1$ mRNA levels increased, so did the levels of cyclin D. We hypothesized that calcium influx through the T-type channel may play a role in the initiation of cyclin D translocation to the nucleus to initiate the cell cycle.

A pharmacological block of $Ca_v3.1$ was achieved using mibefradil, a selective T-type Ca^{2+} channel blocker at micromolar concentrations. PSMCs were plated on 12 mm cover slips, arrested, and treated with 10 μ M mibefradil. In this study there was a control group that was kept in no serum, a group treated with mibefradil alone and no serum, a group treated with 10% FBS, and finally a group treated with mibefradil and 10% FBS.

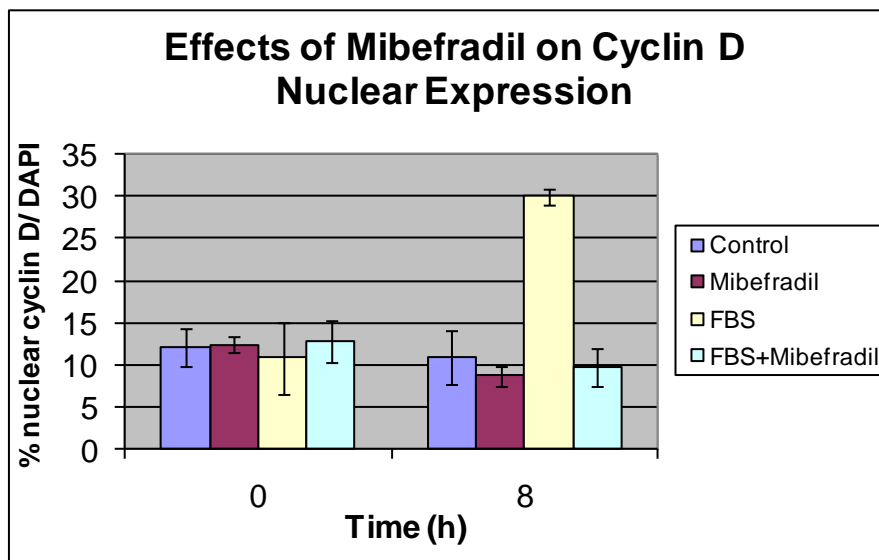


Figure 9. Effect of Mibefradil on cyclin D nuclear translocation.

PASMCs were plated on 12mm cover slips. 4 groups were established: Control (no serum), mibefradil (10 μ M), 10%FBS, and 10%FBS+mibefradil(10 μ M). The groups treated with mibefradil were pretreated for 30 minutes prior to FBS addition. PASMCs were carried out to indicated time points fixed, permeabilized, and stained with monoclonal antibody against cyclin D at a dilution of 1:400. SEM Values- Control T=0 12.3 \pm 2.23, mibefradil T=0 12.7 \pm .88, FBS T=0 10.9 \pm 4.256 FBS+mibefradil T=0 12.7 \pm 2.6 Control T=8 10.4 \pm 3.2, mibefradil T=8 9.7 \pm 1.24 FBS T=8 30 \pm .89 FBS+mibefradil T=8 10 \pm 2.328.

The groups treated with mibefradil were pretreated with 10 μ M of the drug for 30 minutes. Results indicate that mibefradil acted as a potent inhibitor of cyclin D translocation (Figure 9). PSMCs in the treatment group with FBS+mibefradil showed very few cells with cyclin D nuclear expression. At time 0 ~13% of the cells within the

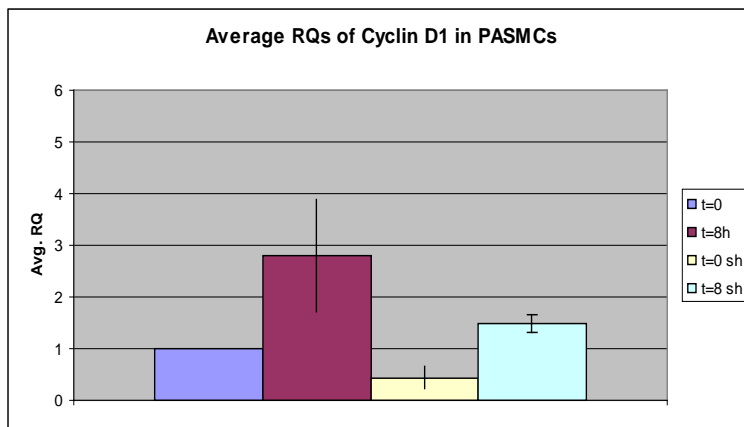


Figure 10. Effects of IGF-1 on cyclin D mRNA levels at 8 hours when treated with Adv-Ca_v3.1sh.

Average of the cyclin D RQ's from 4 passages. RQ values were calculated using T=0 Adv-SCR as the calibrator. Error bars are SEM. A one way ANOVA was used for statistics (p=.402)

population expressed cyclin D intranuclear; after 4 hours the percentage was 12%, and finally at 8 hours after treatment, 9.6% of the cells expressed cyclin D within the nucleus.

This result indicated that treatment with mibefradil was able to block the nuclear expression of cyclin D, which was seen at 30% in populations treated with 10% FBS alone. To further explore this connection, Adv-Ca_v3.1sh was used to knockdown the 3.1 subunit of the T-type channel (previously constructed and validated for Ca_v3.1 knockdown by Dr. F. Pluteanu). In order to confirm that the knockdown was due to the Adv-Ca_v3.1sh and not because of the infection itself, a nonsense virus, "Adv-SCR"

(scrambled target sequence), was used as control. qRT-PCR results confirmed that Adv-Ca_v3.1sh at 8 hours post IGF-1 stimulation resulted in substantial knockdown of Cav3.1 (Figure 10) while Adv-SCR had no significant effect on Ca_v3.1 mRNA level (not shown).

Ca_v3.1 Knockdown and Cyclin D localization in PSMC. Immunostaining was one method used to examine the relationship between T-type Ca²⁺ channels and cyclin D localization. PSMCs were plated on cover slips and infected with either Adv-Ca_v3.1sh for the T-type subunit Ca_v3.1 or with Adv-SCR that served as control. The PSMCs were then arrested and stimulated with IGF-1. Cells were fixed at 0, 4, 8, and 24 hours post stimulation and stained for cyclin D (Figure 11A).

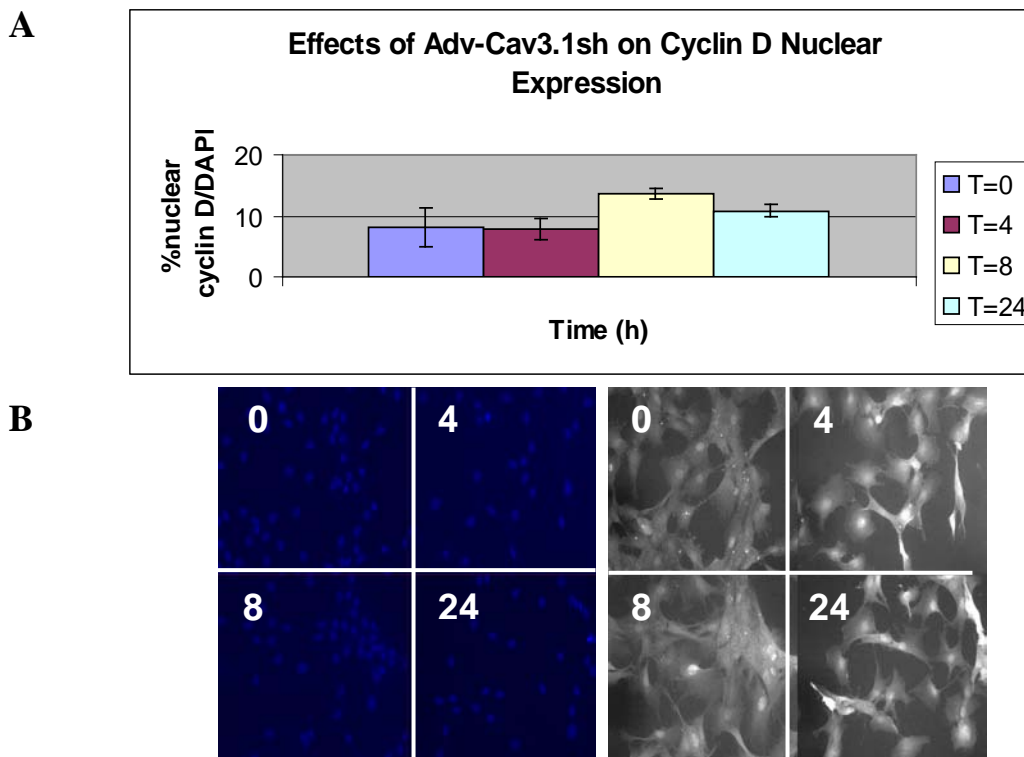


Figure 11. Effect of Adv-Ca_v3.1sh on cyclin D nuclear localization.

(A) Graph represents n=5 studies from different passage numbers 5-7. PSMCs infected with Adv-Ca_v3.1sh for 5 days. Conditions were the same as stated in Figure 4 but cells stimulated with 100ng/μL IGF-1. SEM Values T=0 9.8± 3.21, T=4 9.9± 1.63, T=8 12.3± .932, T=24 10.2± 1.04. (B) Representative micrograph of nuclear DAPI stain (blue) and Cyclin D fluorescence in at the indicated time points.

With Cav3.1 knockdown, cyclin D staining is found predominantly in the cytoplasm compared with images from control panels. As evidenced by the qRT-PCR data, Adv-Ca_v3.1sh significantly knocks down the T-type subunit 3.1 but since the mRNA degradation is time dependent not all mRNA is eradicated from every cell within a population at 5 days post infection. Perhaps that is why we still a few cells that express cyclin D within the nucleus. It must be noted though that the percentage of nuclear localization is greatly reduced compared to control. At time 0 in the control population 12 % of cells expressed cyclin D within the nucleus compared to 8.2% for the Adv-Ca_v3.1sh treated cells. At 4 hours post IGF-1 stimulation in the control condition 12.6% of the cells expressed cyclin D within the nucleus while only 7.8% was seen in the Ca_v3.1 knockdown populations. The most striking contrast can be seen in the 8 hour post stimulation population, the time at which cyclin D nuclear expression was previously shown to be maximal (Figure 5). At 8 hours post IGF-1 treatment in the control samples, 31% of the cells expressed cyclin D in the nucleus while in the Ca_v3.1 knockdown population, 13.6% expressed cyclin D within the nucleus. This represents greater than a 50% reduction in the nuclear expression of cyclin D (Figure 11B).

Using samples from PSMCs previously infected with Adv-Ca_v3.1sh or Adv-SCR and stimulated with IGF-1 (F. Pluteanu), we also examined how the cyclin D mRNA levels may be affected with Ca_v3.1 knockdown. Cultures were infected with Adv-Ca_v3.1sh for 5 days, arrested, and then stimulated with IGF-1. mRNA was isolated at 8 and 24 hours after IGF-1 treatment. As seen in figure 10, Adv-Ca_v3.1sh showed an

average RQ value of $.25 \pm .145$ of the $\text{Ca}_v3.1$ subunit of the T-type channel. With this knockdown, cyclin D mRNA levels at 8 hours were also greatly reduced, 1.3 fold when compared to the levels of mRNA in the control (Adv-SCR) population at the same time points. Another point to note is that these results are consistent with our evidence of the time course of cyclin D nuclear expression. We saw an increase in mRNA levels at time 8 hours post stimulation which matches our results from the immunostaining studies. When the T-type was knocked down using Adv- $\text{Ca}_v3.1\text{sh}$ the cyclin D mRNA was greatly reduced.

To further investigate the importance of T-type Ca^{2+} channel expression in cyclin D nuclear translocation, we employed the Adv-cycD-GFP reagent. PSMCs were plated on 15 mm cover slips and allowed to attach for 24 hours. The cells were then infected with the Adv-cycD-GFP virus. After 24 hours one population of PSMCs was infected with Adv- $\text{Ca}_v3.1\text{sh}$, another with Adv-SCR, and one remained only infected with Adv-cycD-GFP. The Adv- $\text{Ca}_v3.1\text{sh}$ and Adv-SCR treated populations were allowed to incubate for 5 days to ensure proper knockdown of the $\text{Ca}_v3.1$ subunit (Adv-SCR for control). PSMCs were then arrested for 48 hours. Following the arrest, 10%FBS was added back into the media and the cells were placed in the incubator for 3 hours. Cover slips were then mounted in a heating chamber and bathed in HAMs F-12 + 10%FBS. Time lapse photos were taken every 2 minutes to track the translocation of cyclin D. Infection with the Adv- $\text{Ca}_v3.1\text{sh}$ and the Adv-SCR were confirmed at the time of serum addition by photos taken with red filter to visualize the dsRed portion of the

adenoviruses. Nuclear translocation was not observed in our studies under any of the conditions. Translocation did occur but the movement was from the nucleus to the cytoplasm in every condition (Figure 12, Adv-SCR not shown).

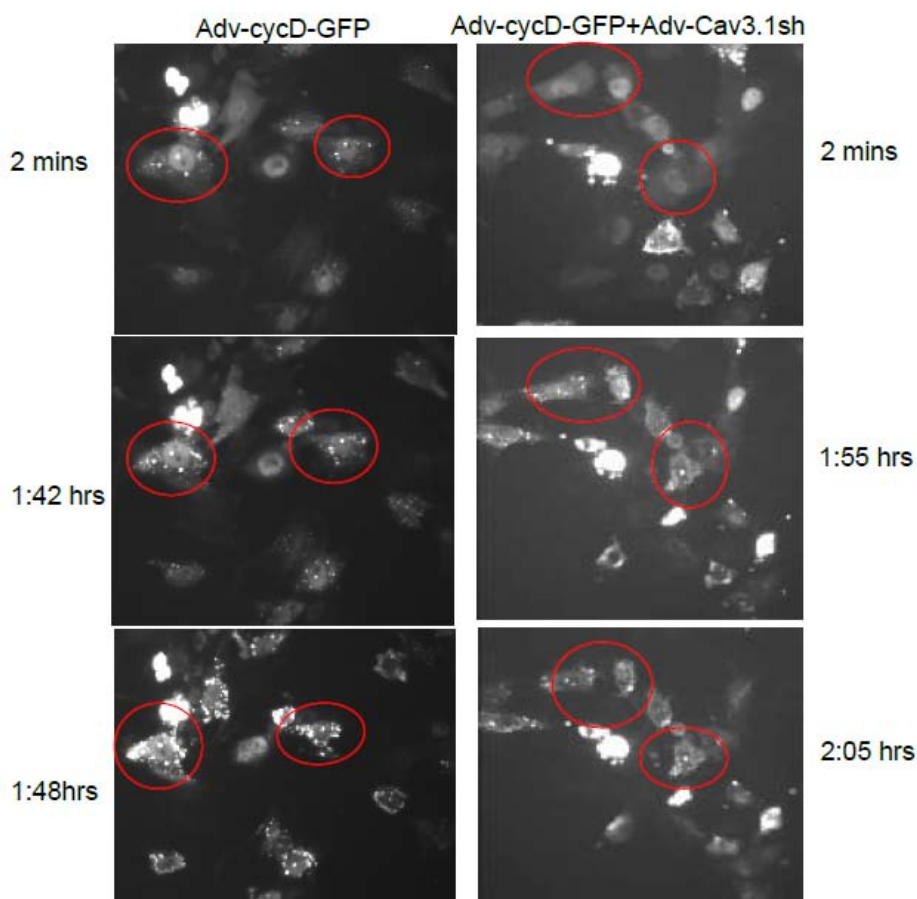


Figure 12. Panels of Time Lapse PSMC Adv-cycD-GFP. PSMCs plated on 15 mm cover slips and infected with Adv-cycD-GFP for 24 hours. Cultures were arrested for 48 hours and stimulated with 10% FBS. PSMCs were placed in 37C incubator for 3 hours prior to time lapse. After 3 hour incubation cover slips were placed in heating chamber and media was changed to HAMs F-12 with 10%FBS. Images were acquired every 2 minutes. Adv-cycD-GFP infected PSMCs. Panel is composed of images acquired at indicated times. Adv-cycD-GFP + Adv-Cav_{3.1}sh. Panel is composed of images acquired at indicated times.

CHAPTER 4

DISCUSSION

Our experiments set out to determine a relationship between cyclin D and T-type calcium channels. Previous studies have provided evidence (Dr Pluteanu, 14) that the same factors, for example mitogenic factors, effect the regulation of both the channels and cellular proliferation but an association between the two has yet to be established.

The first experiments were set up to determine a base line for cyclin D activity, namely its translocation to the nucleus to begin the cell cycle. Since data had been presented to suggest that T-type channel mRNA is increased with serum and IGF-1, studying the effects on cyclin D translocation seemed the logical step. Our results confirm the upregulation of the $Ca_v3.1$ subunit of the T-type channel as well as confirm the mitogenic effects of proliferation on PSMCs. Immunostaining, western blot, and qRT-PCR allowed us to determine the time course for cyclin D nuclear expression. While results from immunostaining suggest that translocation of cyclin D protein may occur at 8 hours post stimulation, results from qRT-PCR show an insignificant increase in cyclin D mRNA levels at 8 hours. The absence of cyclin D mRNA upregulation at 8 hours may be due to the cycling of the cyclin D mRNA itself and the translocation that was observed may be do to protein that had been made earlier than the 8 hour time point. Previous

studies have suggested a half life of 30 minutes for the cyclin D protein so perhaps the mRNA is being made but degraded or perhaps is not stabilized. Further studies where PASMCM mRNA could be isolated at closer time points after stimulation may prove beneficial in better understanding how cyclin D mRNA levels relate to protein expression and movement. Since variability was seen within the populations isolated, more experiments should be done.

Western blot analysis was performed in where the cells underwent fractionation of the cytosolic and nuclear fractions. The western seems to confirm our time course of translocation for 0, 4, and 24 hours after stimulation but at 8 hours cyclin D appears to be more cytosolic when nuclear translocation was expected to be observed based on our previous data. Based on the lamin lanes, it should be noted that fractionation was not pure which may have lead to the results obtained. This experiment was performed only once so more westerns would need to be run in order to reach a conclusion. Due to the variability observed in many of our studies cell sorting by FACS analysis may be a useful technique in order to better elucidate the time course of cyclin D translocation. A western blot looking at the protein levels of $Ca_v3.1$ was unable to be performed do to the lack of specificity of our $Ca_v3.1$ antibody.

Once our theory of base line cyclin D activity had been established we set out to better understand the interplay between the T-type channel and cyclin D translocation when the channel was knocked down. Previous studies have shown the effectiveness of mibefradil, a pharmacological T-type channel blocker, on the channel so studies were performed to corroborate this data as well examine the knockdown of the T-type channels

effects on cyclin D. Immunostaining results suggest that mibefradil was able to block the T-type channel do to the low percentage of cells with cyclin D nuclear expression after treatment. For the immunostaining experiments, cell populations received 10 μ M of mibefradil which was suitable to block the T-type channel based on electrophysiology findings performed by Dr F. Pluteanu (data not shown). While the nuclear expression of cyclin D seemed to be blocked with this knockdown, it should be stated that cells did not survive past 24 hours of treatment with mibefradil. To further confirm our data, qRT-PCR should be done to confirm that the $Ca_v3.1$ channel was knocked down while the L-type channel was unaffected.

Since the specificity of pharmacological agents for T-type channels is low, small hairpin RNAs were designed in our lab to directly target the mRNA of $Ca_v3.1$ and silence the gene. Immunostaining results indicated interplay with cyclin D and the T-type channel based on the data that the percentage of cells with nuclear expression of cyclin D was greatly reduced at every time point with treatment with Adv- $Ca_v3.1$ sh. Our qRT-PCR results also show a slight reduction in cyclin D mRNA levels, specifically at 8 hours post stimulation but were not significant (Figure 10). mRNA levels of cyclin D as well as $Ca_v3.1$ were unaffected by the nonsense virus, Scramble, used as control (Figure 10).

In order to visualize the movement of cyclin D within PASMCs, cyclin D was fused to a GFP and inserted into an adenovirus. It should be noted that with this construct over expression of exogenous cyclin D is observed and may behave differently than endogenous cyclin D. After the Adv-cycD-GFP was made, HEK cells were infected

either with GFP alone or with Adv-cycD-GFP, which was found in the nucleus. Based on this result, time lapse experiments were set up and PASMCs were infected with; Adv-cycD-GFP, Adv-cycD-GFP plus Adv-Ca_v3.1sh, or Adv-cycD-GFP plus Adv-SCR. There were many limitations for these experiments including that the cells could only be placed in the heated chamber for 2 hours before dying. The time lapse experiment was performed twice and more studies must be done in order to gain a better understanding of the effects of Adv-Cav3.1sh on the translocation of cyclin D.

The scope of this thesis was limited to the study of cyclin D because it is one of the earliest players in the cell cycle but future experiments may want to look at downstream proteins such as other cyclins or CDKs and their possible involvement with the T-type channel. Serum stimulation and IGF-1 were the only mechanisms of proliferation studied so the scope of mitogenic factors that influence the interaction between the T-type channel and cyclin D translocation could be broadened.

The T-type channel is comprised of 3 subunits, only 2 of which were studied in this paper. Mibefradil targets the Ca_v3.1 and 3.2 subunits displaying preference for Ca_v3.1 but using pharmacological blockers is not the best option for blocking these channels since the drug has a propensity to also block L-type channels. qRT-PCR data confirms the knockdown of the Ca_v3.1 mRNA using Adv-Ca_v3.1sh (Figure 10) which suggested the involvement of T-type channel with cyclin D regulation but the Ca_v3.2 subunit was not directly addressed. Previous studies performed by Dr Pluteanu showed that serum and mitogenic factors do not seem to have a direct effect the Ca_v3.2 subunit

(Figure 2B) and hence were not directly studied in this thesis project. While the data presented suggest a correlation between the T-type and cyclin D regulation many other players are yet to be studied. The role of calmodulin and calcineurin could be looked at as possible intracellular calcium messengers and their interaction with cyclin D or if a relationship exists with the T-type channel. As previously stated cyclin D is an earlier player in the cell cycle but even cyclin D is a down stream target of many pathways including the MAPK/ERK and PI3 pathways (20). Studying players in this pathway may serve as a mechanism to better understand smooth muscle proliferation.

CHAPTER 5

CONCLUSIONS

From the studies performed in this thesis a few conclusions may be drawn. The evidence provides a theory that T-type calcium channels are involved in the activation but not the transcriptional regulation of cyclin D. Meaning that the channels may be involved in the movement and subsequent activation of the cyclin D protein itself and not in its transcriptional regulation. qRT-PCR studies provided little evidence of a direct correlation between T-type channel upregulation and the upregulation of cyclin D mRNA levels. There may be a trend but more studies are required to elucidate a connection. The experiments that make the case for this conclusion are the mibefradil studies as well as the immunostaining studies performed when cultures were infected with Adv-Ca_v3.1sh. Results from both of these studies indicate that the T-type channel is needed for the nuclear expression of cyclin D, indicating that the channel allows the cyclin D protein to translocate into the nucleus. The mibefradil as well as the Adv-Ca_v3.1sh studies show a marked reduction in nuclear expression of cyclin D post stimulation, specifically at 8 hours. More studies may be necessary to determine the exact relationship between the T-type channel and cyclin D such as western blot analysis examining the expression of cyclin D within the nucleus following the knockdown of the T-type channel.

CHAPTER 6

FUTURE STUDIES

Future studies to perform would be cell sorting by FACS which would allow us to determine just how many cells in a population are undergoing which specific stage of the cell cycle. Also other mitogenic factors should be examined for their effect on both the T-type channel and cyclin D, for example thyroid hormone (T3) which has been shown to induce cyclin D nuclear translocation (11). Future experiments should also start to look at how some of the down stream players are affected under the same experimental conditions performed in this thesis such as cyclin E and A, which are cyclins required for the transition between G₁/S phase and G₂/M phases respectively. In order to clarify how cyclin D mRNA levels affect protein expression, mRNA should be isolated at closer time intervals. Finally, performing cytosolic vs. nuclear fraction western blots with populations infected with Adv-Ca_v3.1sh and Adv-SCR would help clarify the role of the T-type channels' involvement with cyclin D nuclear translocation.

BIBLIOGRAPHY

1. Brueggemann L, et al., Low voltage-activated calcium channels in vascular smooth muscle: T-type channels and AVP-stimulated calcium spiking. *Am J Physiol Heart Circ Physiol.* 2005, 288: H923–H935
2. Cribbs L.L. Vascular Smooth Muscle Calcium Channels. Could “T” be a Target? *Circulation Research Journal of the American Heart Association.* 2001;89;560-562.
3. Choi J, Chiang A, Taulier N. A Calmodulin-Binding Site on Cyclin E Mediates Ca²⁺-Sensitive G1/S Transitions in Vascular Smooth Muscle Cells. *Circulation Research Journal of the American Heart Association.* 2006;98:1273-1281
4. Chuang, R.S., et al., Inhibition of T-type voltage-gated calcium channels by a new scorpion toxin. *Nat. Neurosci.* 1998, 668-674
5. Kahl, C. et al. Regulation of Cell Cycle Progression by Calcium/Calmodulin-Dependent Pathways. *Endocrine Reviews.* 2003; 24(6): 719-736
6. Kapur, N. et al. Cell cycle-dependent calcium oscillations in mouse embryonic stem cells. *AJP-Cell Physiology.* 2006; 292: 1510-1518.
7. Kato, J. et al. Regulation of cyclin D-dependent kinase 4 (cdk4) by cdk4-activating kinase. *Mol Cell Biol.* 1994 April; 14(4): 2713–2721.
8. Koledova V, Khalil R. Ca²⁺, Calmodulin, and Cyclins in Vascular Smooth Muscle Cell Cycle. *Circulation Research Journal of the American Heart Association.* 2006;98:120-1243
9. Krzysztow, R et al. Insulin-like Growth Factor-1 Receptor and Its Ligand Regulate the Reentry of Adult Ventricular Myocytes into the Cell Cycle. *Experimental Cell Research* 1997; 235, 198-203
10. Kuemmerle, J. et al. IGF-I stimulates human intestinal smooth muscle cell growth by regulation of G1 phase cell cycle proteins. *Am J Physiol Gastrointest Liver Physiol* 2004 286: G412–G41

11. Ledda-Columbano, Giovanna M. et al. Thyroid hormone induces cyclin D1 nuclear translocation and DNA synthesis in adult rat cardiomyocytes. *FASEB J.* 2006, 20, 1, 87-94
12. Leone, G. et. al. E2F3 activity is regulated during the cell cycle and is required for the induction of S phase. *Genes Dev.* 1998;12: 2120-2130
13. Mateyak, M.K. et. al. c-Myc regulates cyclin D-Cdk4 and -Cdk6 activity but affects cell cycle progression at multiple independent points. *Mol. Cell Biol.* 1999;19: 4672-4683.
14. McLatchie, L. et al. Are T-type calcium channels causally involved in neonatal cardiac myocyte hypertrophy? *Journal of Physiology and Experimental Physiology* 2005; 565: 24-33
15. Nuss, HB. Houser, SR. T-type Ca²⁺ current is expressed in hypertrophied adult feline left ventricular myocytes. *Circulation Research.* 1993;73:777-782
16. Rasmussen, C. Rasmussen, G. Calmodulin-dependent protein kinase II is required for G1/S progression in HeLa cells. *Biochem Cell Biol.* 1995 Mar-Apr;73(3-4):201-7
17. Rodman, D. et al. Low-Voltage-Activated (T-Type) Calcium Channels Control Proliferation of Human Pulmonary Artery Myocytes. *Circ Research.* 2005;96;864-872
18. Santella L. The Role of Calcium in the Cell Cycle: Facts and Hypotheses. *Biochemical and Biophysical Research Communications.* 1998; 244: 317-324.
19. Short, A. et al. Intracellular Ca²⁺ pool content is linked to control of cell growth. *Proc Natl Acad Sci* 1993 90:4986-4990
20. Takuwa, N et al. Cyclin D1 Expression Mediated by Phosphatidylinositol 3-Kinase through mTOR-p70s6k-Independent Signaling in Growth Factor Stimulated NIH 3T3 Fibroblasts. *Mol Cell Biol* 1999 19: 1346-1358.
21. Yokoyama U, Minamisawa, et al. Multiple transcripts of Ca²⁺ channel α 1-subunits and a novel spliced variant of the α 1C-subunit in rat ductus arteriosus. *Am J Physiol Heart Circ Physiol* 2006: 290:1660-1670.

VITA

I am originally from Omaha, Ne. I left after I graduated from Marian High School, 2001, to attend Emory University in Atlanta, GA. I received a BS in Biology May of 2005. After graduation I spent a year abroad volunteering in an intercity hospital in Mexico City. Upon my return I began my Master's studies in Cellular and Molecular Physiology at Loyola University of Chicago. I defended my thesis in April of 2008. I am currently a Physician Assistant student at the University of Kentucky with plans to graduate in May 2012.

THESIS APPROVAL SHEET

The thesis submitted by Abigail Prier has been read and approved by the following committee:

Leanne Cribbs, Ph.D.
Associate Professor of Medicine and Physiology
Loyola University Chicago

Jody Martin, Ph.D.
Associate Professor of Medicine and Physiology
Loyola University Chicago

Allen Samarel, M.D.
Professor of Medicine
Loyola University Chicago

The final copies have been examined by the director of the thesis and the signature which appears below verifies the fact that any necessary changes have been incorporated and that the thesis is now given final approval by the committee with reference to content and form.

The thesis is therefore accepted in partial fulfillment of the requirements for the degree of Master of Science.

Date

Director's Signature